Boletim da Sociedade Astronômica Brasileira, **34**, no. 1, 231-232

Gradient Pattern Analysis of the Solar Active Region NOAA 11131

R. A. Sautter[1], R. R. Rosa[1], R. Sych[2], H. S. Sawant[1], & S. K. Bisoi[3]

[1] National Institue for Space Research e-mail: rubens.sautter@inpe.br
[2] Institute of Solar-Terrestrial Physics SB RAS e-mail: sych@iszf.irk.ru
[3] National Institute of Technology Rourkelae-mail: susanta@nao.cas.cn

Abstract. Analyzing the evolution of active solar regions is extremely important not only in the scope of solar physics but also in the monitoring of solar activity for a better understanding of space weather. In this work, we present results from the application of the technique known as Gradient Pattern Analysis (GPA) to study the dynamics of an active region NOAA 11131 during a class X flare. The GPA technique allows the detection of bilateral symmetry breaks in the gradient field of a spatiotemporal snapshot sequence. The results, based on the fluctuation of norms and phases of the gradient field, are able to detect extreme fluctuations in the space-time domain, which are compatible with the maximums measured in SFU. The variation of the spectral indices, via the Power Spectrum Density, concatenated with the fluctuation of the asymmetries extremes, indicates an absorption in the periodicity of 2.5 minutes. The periodicity of 3 minutes has been already evidenced in other works, where the authors propose that these source dynamics are the result of wavefronts along the loops extending outwards from magnetic bundles of the umbra.

Resumo. Analisar a evolução das regiões solares ativas é extremamente importante no âmbito da física solar, para uma melhor compreensão do clima espacial e monitoramento da atividade solar. Neste trabalho apresentamos resultados da aplicação da técnica conhecida como Análise de Padrões do Campo Gradiente (cujo acrônimo em inglês é GPA) para estudar a dinâmica de uma região ativa durante um evento solar de classe X. Dado uma sequência de imagens, a técnica GPA permite a detecção de quebras de simetria bilaterais do campo gradiente das imagens. Os dados analisados consistem em uma observação obtida por meio do Solar Digital Observatory (SDO) da região ativa NOAA 11131. Os resultados, baseados na flutuação de normas e fases do campo gradiente, indicam flutuações extremas no domínio do espaço-tempo compatíveis com os máximos medidos em Unidades de Fluxo Solar (cujo acrônimo em inglês é SFU). A variação dos índices espectrais, provenientes da flutuação das assimetrias medidas ao longo do tempo, indicam uma absorção de energia em um período de 2.5 minutos. Trabalhos relacionados a esta região ativa indicam a periodicidade de 3 minutos, onde os autores propõem que a dinâmica periódica provém dos feixes magnéticos da umbra.

Keywords. Techniques: image processing – sunspots – Sun: oscillations

1. Introduction

The solar corona seismology is essential to understand the sunspot's formation and evolution. The most recent studies investigate the oscillations of magneto-acoustic waves of 5 minutes and 3 minutes. There are several candidate models to explain these dynamics (Cho et al. 2019; Felipe 2019), whose hypotheses are related to small-scale plasma convection or the cutoff frequency of a p-mode. We investigate the NOAA 11131 since it is a standard observation for a 3-minutes sunspot oscillatory dynamic (Deres & Anfinogentov 2015; Sych, Jess & Su 2021; Sych et al. 2012). The region was observed on December 10, 2010, by the Solar Digital Observatory (SDO). From the sunspot's images, the umbra at 304 Å was tracked over 6 hours, with 12 seconds of time resolution, using the methodology proposed by Sych et al. (2012). To complement the previous studies of NOAA 11131, we introduce the Gradient Pattern Analysis (GPA)[1]. This technique provides a set of morphological metrics related to spatial gradient symmetry. The observation over time of GPA metrics combined with subsequent time-series analysis can describe the transient stages and oscillatory characteristics induced by the underlying solar physics.

2. Gradient Pattern Analysis

The GPA paradigm characterizes patterns according to the spatial fluctuation of amplitudes, namely the Gradient Field (GF) (Rosa, Sharma & Valdivia 1998, 1999; da Silva et al. 2000; Assireu et al. 2002; Andrade, Ribeiro & Rosa 2006). In this way, the analysis is sensitive to perturbations and invariant to the image amplitude average. The technique establishes gradient symmetry and gradient moment concepts to characterize GFs. The former concept has been a topic of a recent study (Rosa et al. 2018), which determines critical regions in patterns. The Asymmetric Gradient Method (AGM) classifies vectors into symmetrical or asymmetrical according to a neighborhood of points equally distant from the image center. A given vector is symmetrical if it has at least one neighbor with the same modulus and opposite phase, otherwise, it is asymmetrical. Figure 1 have some examples of sunspot's gradient symmetry segmentation. The regions which are associated with instabilities are usually asymmetrical. Therefore, the following steps of the technique contemplate features of the asymmetrical vectors.

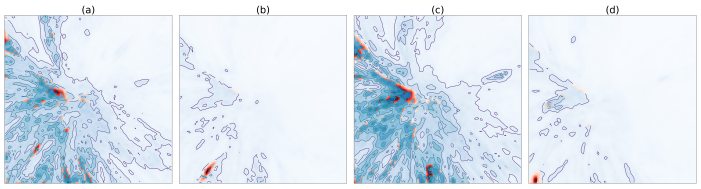

Figure 1. Snapshots of NOAA 11131 observed regimes: after the former extreme peak (a), at the first extreme peak (b), in between extremes (c), and at the second extreme peak (d). With the analysis of GPA, it has been detected gradient symmetrical regions, which are presented in blue, and gradient asymmetrical regions which are in red.

[1] https://github.com/rsautter/GPA

Pattern analysis usually requires several metrics to represent its main characteristics. However, the conjunction of similar metrics reinforces redundant information; that can contaminate the following analysis steps. Thus, every metric is related to a Gradient Moment (GM) in GPA formalism (Rosa et al. 2003). The first Gradient Moment (GM1) is the geometrical representation of the gradient field, which comprises information about the position, modulus, and phases of each vector in the gradient field.

In this context, the Delaunay triangulation of the induced space can enclose all characteristics of GM1, where the induced space is formed by the sum of each vector with its corresponding position. For a set of Delaunay triangulation connection lengths L, we propose the metric:

$$G_1 = \frac{\overline{L}_{sup} - \overline{L}_{inf}}{\max(L)}, \tag{1}$$

where $\overline{L}_{inf}$ is the average of connections that are smaller than the overall set average, and $\overline{L}_{sup}$ is the average of the set higher than the overall set average. Thus, the more diverse the Delaunay triangulation lengths, the higher G_1.

Subsequent GM carries information about a single characteristic of the GF to enhance aspects that are not evident in GM1. For instance, GM2 comprises the GF modulus information, whereas GM3 contains information from the phases. In this sense, Rosa et al. (2018) proposes the following metric for GM2:

$$G_2 = \frac{V_A}{V}\left(1 - \frac{\left|\sum_{i=0}^{V_A} v_i\right|}{2\sum_{i=0}^{V_A}|v_i|}\right), \tag{2}$$

that is a ratio between the global vector field $|\sum v_i|$ and every asymmetrical vector modulus $|v_i|$. The metric also contains the proportion of the number of asymmetrical vectors V_A in relation to the total number of vectors V. Therefore, the metric approaches its maximum value with incoherent patterns. For instance, in a context of vectors in all directions, $|\sum v_i| = 0$, and therefore $G_2 = V_A/V$. However, if all vectors are aligned, then $|\sum v_i| = V_A|v_i|$, thus $G_2 = V_A/(2V)$.

Finally, we propose the following metric for GM3:

$$G_3 = \frac{V_A}{2V} + \sum_{i=0}^{V_A} \frac{\cos(\theta_i)\cos(\phi_i) + \sin(\theta_i)\sin(\phi_i) + 1}{4V_A}, \tag{3}$$

which is an operation between the direction ϕ_i of a given vector and the phase θ_i, and the proportion of asymmetrical vectors. The minimum value of this metric is achieved when phases are opposite with their locations since $\cos(\theta_i)\cos(\phi_i)+\sin(\theta_i)\sin(\phi_i) = -1$ in this scenario. On the other hand, the metric is minimum when all vectors are aligned.

Briefly, we described GPA formalism, whose core is the symmetry of the gradient field and the gradient moments. With the presented metrics concatenated over time, we can study the morphological dynamic of the sunspot. The following section describes the application of the technique.

3. Results and Concluding Remarks

The sunspot analysis shows two stages where the asymmetry of the pattern is maximum, as described in Figure 2. The period in which the symmetry breaking occurred, as well as the GMs amplitude, are different in both stages. The first stage has a shorter duration and higher GMs. Furthermore, the spectral analysis of the G_2 signal shows a decline in the Power Spectrum Density (PSD) for 2.5 minutes. In future works, we will investigate the relationship between asymmetry and the periodicity of known standard signals.

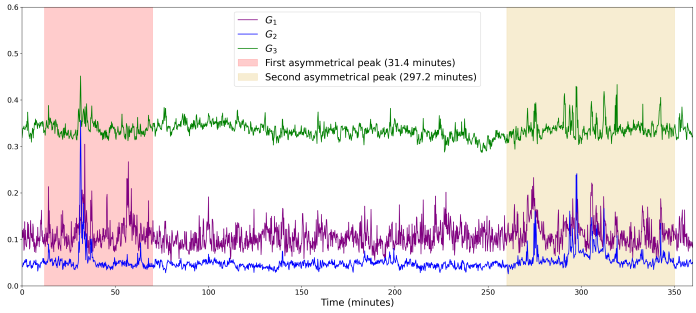

Figure 2. Gradient Moments of NOAA 11131. Red and yellow regions are associated to different extreme GM fluctuation regimes.

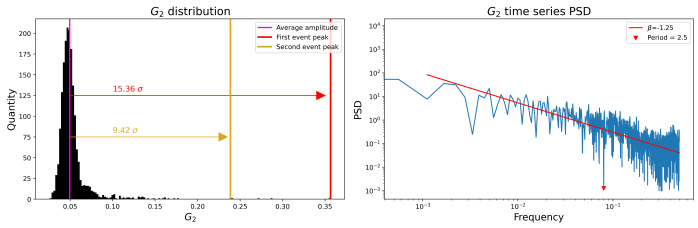

Figure 3. Time series analysis of G_2; the left chart shows the statistical distribution of G_2. The right chart is the Power Spectrum Density (PSD) whose power scaling law is $1/f^{1.25}$, where f is the frequency, and it indicates the absorption of energy at the period of 2.5 minutes.

Acknowledgements. This study was financed in part by the Coordenação de Aperfeiçoamento de Pessoal de Nível Superior - Brasil (CAPES) - Finance Code 001

References

Cho, K., Chae, J., Lim, E. & Yang, H., 2019, The Astrophysical Journal, 879, L101.
Felipe, T., 2019, Astronomy & Astrophysics, 627, A169.
Deres, A. S. & Anfinogentov, S. A., 2015, Astronomy Reports, 59, 959.
Sych, R., Jess, D. B. & Su, J., 2021, Philosophical Transactions of the Royal Society A, 379, 180.
Sych, R., Zaqarashvili, T. V., Nakariakov, V. M., Anfinogentov, S. A., Shibasaki, K. & Yan, Y., 2012, Astronomy & Astrophysics, 539, A23.
Rosa, R. R., Campos, M. R., Ramos, F. M., Vijaykumar, N. L., Fujiwara, S. & Sato, T., 2003, Brazilian journal of physics, 33, 605.
Rosa, R. R., De Carvalho, R. R., Sautter, R. A., Barchi, P. H., Stalder, D. H., Moura, T. C., Rembold, S. B., Morell, D. R. F. & Ferreira, N.C., 2018, Monthly Notices of the Royal Astronomical Society: Letters, 477, L101.
Rosa, R. R., Sharma, A. S. & Valdivia, J. A., 1998, Physica A: Statistical Mechanics and its Applications, 257, 509.
Rosa, R. R., Sharma, A. S. & Valdivia, J. A., 1999, International Journal of Modern Physics C, 10,147.
da Silva, A. F., Rosa, R. R., Roman, L. S., Veje, E. & Pepe, I.,2000, Solid State Communications, 113,703.
Assireu, A. T., Rosa, R. R., Vijaykumar, N. L., Lorenzzetti, J; A., Rempel, E. L., Ramos, F. M., Sá, L. D. A., Bolzan, M. J. A. & Zanandrea, A., 2002, Physica D: Nonlinear Phenomena, 168, 397.
Andrade, A. P. A., Ribeiro, A. L. B. & Rosa, R. R., 2006, Physica D: Nonlinear Phenomena, 223, 139.
Rosa, R. R. and Pontes, J., Christov, C. I., Ramos, F. M., Neto, C. R., Rempel, E. L. & Walgraef, D., 2000, Physica A: Statistical Mechanics and its Applications, 283, 156.